

Improvements in SIMS continue. Is the end in sight?

Nicholas Winograd^a, Zbigniew Postawa^b, Juan Cheng^a, Christopher Szakal^a, Joseph Kozole^a, Barbara J. Garrison^a

^aDepartment of Chemistry, Penn State University, University Park, PA 16802

^bSmoluchowski Institute of Physics, Jagiellonian University, Krakow, Poland, Department of Chemistry

Abstract

Cluster ion bombardment is at the forefront of current ToF-SIMS research, particularly when examining the feasibility of molecular depth profiling and three-dimensional imaging applications. It has become increasingly clear that secondary ion emission after cluster projectile impact results from a radically different sputtering mechanism than the linear collision cascades that dominate after atomic ion bombardment. The new physics involved with cluster ion impacts dramatically change the traditional approaches toward sample analysis with the SIMS technique. Several new ion bombardment properties have emerged from experimental and theoretical work involving cluster ions such as Au_3^+ , Bi_3^+ , SF_5^+ , and C_{60}^+ - all of which are commercially available ion sources. These new properties lead to new rules for traditional static SIMS experiments, provoking new methodologies, and introducing new applications – especially where high mass sensitivity and high-resolution imaging of organic and biological materials are necessary. This paper aims to elucidate recent experimental and theoretical work on these new cluster ion properties and offers insights into how these special properties can be used for future experiments and applications.

Keywords: ToF-SIMS, Cluster ion, Au_3^+ , SF_5^+ , C_{60}^+

1. Introduction

Throughout the long history of secondary ion mass spectrometry research, the field has evolved along two distinct paths. In one instance, ion beams have been employed to desorb elemental species from the surface of materials¹. To enhance the formation of atomic ions, the electronic properties of the system have been tuned using special ion beams such as Cs or O_2^+ . The strategy is largely successful, with useful yields exceeding 10% in many cases. By utilizing high ion fluence and focused atomic ion probe beams, three-dimensional elemental analysis has been feasible. The state of dynamic SIMS is highly advanced, with many routine applications in materials science and electronics now established.

The second path, the use of SIMS to characterize molecular surfaces, has been more tortuous. The rapid accumulation of chemical damage created by the incident ion beam creates a limit to the ion fluence³, greatly reducing the amount of material available for detection. Low secondary ion fractions and extensive molecular fragmentation further exacerbate the problem. Several important advances have addressed these issues. Perhaps the most significant development

was the rapid transition from quadrupole detectors commonly employed in the 1970's and 80's to high performance time-of-flight analyzers⁴ now in widespread use. The high transmission and parallel mass measurement properties of these devices increased sensitivity by many orders of magnitude. Another important technical development was the introduction of the liquid metal ion source for TOF experiments, originally utilizing Ga ions⁵. These sources had much greater brightness than gas ion sources, and could be pulsed and focused to submicron probe sizes. Molecule-specific imaging experiments quickly followed, but sensitivity limitations have greatly constrained applications.

Another factor that has indirectly influenced the development of molecular SIMS has been the widespread adoption of matrix-assisted laser desorption ionization (MALDI) mass spectrometry⁶. Although the unprecedented success of this technique for the assay of high molecular weight molecules (i.e. peptides and proteins) has focused the attention of the enormous biological community on desorption mass spectrometry approaches, the reduced fragmentation and almost unlimited mass range of MALDI has extended its applications well beyond the biological field. The high lateral resolution imaging properties of SIMS along with its surface sensitivity have not been sufficient to make significant inroads into the biological community.

The development of cluster ion beams offers the possibility to change this balance and to allow molecular SIMS to approach the same or greater degree of sophistication now associated with dynamic SIMS. Interestingly, it has been known at least since 1989 that cluster bombardment greatly enhances the yield of molecular ions⁷. During the 1990's, interest in the use of these sources continued with the commercial introduction of an SF₅⁺ source. Although the number of cluster bombardment papers at these International SIMS conferences continued to rise for a few years, there were only 4 such talks at the Nara conference in 2001⁸. Perhaps the difficulty in implementation of these devices inhibited widespread use, even if the advantageous properties were recognized. In addition, some systems showed no enhancement while others showed huge enhancements. The lack of rationale for these differences confused the field. At the Nara conference, the discussion centered around the use of a gold cluster liquid metal ion source⁹ and a gas C₆₀⁺ source¹⁰ that could be focused to a probe size of a few microns. Both of these sources were commercialized and the LMIG was rapidly adopted by the community. The C₆₀ source was shown to exhibit superior SIMS spectra in most cases, but its poorer imaging quality and expense probably slowed acceptance. In any case, at this conference (SIMS XV) about 20% of all the presentations, nearly 70 in total, utilize cluster SIMS in some fashion. In just 4 years, the field has changed enormously.

With more players come more results. New rules for the implementation of cluster SIMS are emerging that suggest it may complement MALDI experiments in many research domains. For example, the physics of the cluster solid interaction has a mesoscopic character that is of a size between the collision cascades associated with atomic bombardment and the macroscopic ablation phenomenon associated with MALDI. Many groups have shown that the static limit can be ignored using cluster bombardment and that molecular depth profiling is possible¹¹⁻¹⁷. C₆₀⁺ sources with submicron probe sizes are now available for imaging¹⁸. Fundamental measurements suggest the sputtering yield of organic materials can be very high – several hundred to several thousand molecules per projectile^{11, 14}, and that the molecular ion yield can also be enhanced by a built-in chemical ionization mechanism. Under the proper circumstances, cluster bombardment also reduces the formation of topography during sputtering¹⁹, improving the prospects for depth profiling of multilayers with little interlayer mixing. All of these observations have major implications for improved imaging experiments because of the increased amount of material available for analysis.

Here we examine some of these emerging new rules by comparing molecular dynamics computer simulations of cluster bombardment to newly acquired experimental data from our laboratory on both organic and inorganic materials. Although the story is by no means complete, several general principles are presented to hopefully guide future experiments where sensitivity and mass range are critical issues.

2. A View from Computer Simulations

Over the years we have performed many computer simulations aimed at understanding ion bombardment of solids. At times the simulations have been designed to model very specific systems and very specific phenomena. At other times the simulations provide only a mental picture of how to think about the experimental data. In the following section, primarily calculations of Ga and C₆₀ bombardment of a Ag single crystal are presented. We acknowledge that Ag is quite different from many of the substrates discussed in **Section 3**. The suggestions made by these simulations, however, have aided all of us immensely in interpreting the experimental results even though the materials are dissimilar.

2.1. New Physics of Cluster Bombardment

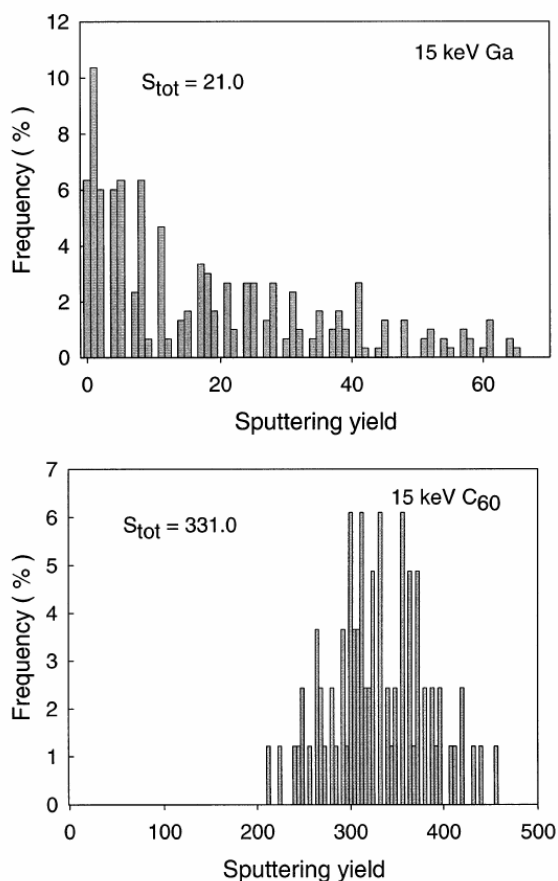


Fig. 1. The relative frequency of impacts leading to a given sputtering yield for 15 keV Ga and C₆₀ projectiles on a Ag{111} surface at normal incidence²⁰.

The bombardment of solids by cluster beams has introduced a new mechanism for the ejection of material in SIMS. The atomic bombardment process can be visualized as a sophisticated game of pool or billiards. That is, individual atoms collide with individual atoms. As in a pool game, there is a great diversity of the types of motion that can occur. One way of representing this diversity is to plot the frequency that a given number of particles eject per incident ion. Shown in Figure 1 is the distribution for 15 keV Ga bombardment on Ag{111}.²⁰ There is a wide spread in the number of particles ejected from zero to over 60 with an average sputtering yield, S_{tot} , of 21. The large frequencies for the small (or zero) number of ejected particles means that many atomic ions that strike the surface are completely wasted in terms of providing useful SIMS signal. In contrast, the bombardment of Ag{111} by C₆₀ results in a relatively narrow distribution about a

much higher yield as shown in Figure 1. In this case the total yield is 331 and the minimum number of ejected particles is over 200. In other words, *every* C₆₀ particle is providing more potentially useful signal than *any* of the individual Ga particles.

The first two big concepts that arise from the information displayed in Figure 1 are as follows:

- Cluster bombardment can greatly enhance the yield over atomic bombardment. The amount of enhancement, if any, of course depends on the precise nature of the cluster beam and the substrate. Thus, as initially proposed by Appelhans and Delmore,⁷ there is potential for enhanced sensitivity that could aid all aspects of SIMS from individual mass spectra to imaging.
- The cluster beam has all incident ions removing similar amounts of material. This point is especially important for imaging applications as there will be uniformity of information throughout the scanning process.

The nature of the resulting solid for Ga and C₆₀ bombardment²¹ of Ag{111} is shown in Figure 2. The two trajectories shown exhibit the average total sputtering yield in each case. The atoms in the substrate are colored by original layer in order to show the mixing that occurs. For the Ga bombardment, the Ga (black) has implanted into the middle of the light blue layer and there is considerable mixing of the upper layers. On the other hand, the C₆₀ projectile has formed a crater and the mixing or disruption is limited to the area immediately surrounding the crater. Most of the C atoms have ejected.

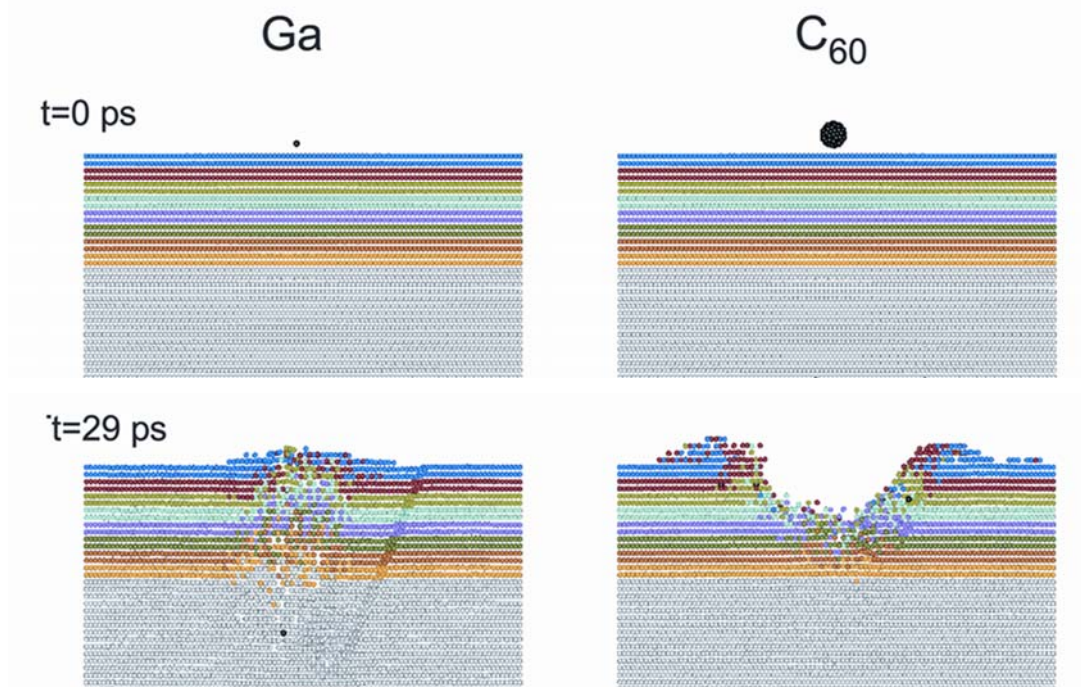


Fig. 2. A cross sectional view of the temporal evolution of a typical collision event leading to ejection of atoms due to 15 keV Ga and C₆₀ bombardment of a Ag{111} surface at normal incidence. The atoms are colored by original layer in the substrate. The projectile atoms are black²¹. Animations of these two trajectories are available on the web at http://galilei.chem.psu.edu/Flicks_post2000.html.

Figure 2 has been the vision diagram for cluster bombardment since Zbigniew Postawa showed it at SIMS XIV²² in San Diego in 2003. The major point is as follows:

- The damage created by C₆₀ is less and more confined than that created by Ga. Even though these simulations are for an atomic solid, the experimental evidence for molecular systems as discussed below follows this vision. In particular, with the high ejection yields with the cluster

bombardment, it is possible to have sufficiently large sputtering yields such that all the damage is removed in the next collision event. This possibility opens the door for molecular depth profiling experiments. The static limit as so often invoked for molecular SIMS has been shattered by the cluster beams.

There is new physics with the cluster bombardment. The C_{60} is larger than the Ga ion and is larger than the spacing between the substrate atoms. This increased size leads to a mesoscale motion that resembles a meteor hitting the earth. The subsequent motion of the particles is not a sophisticated pool or billiards game but rather, it is an organized motion resembling flow from a nozzle²³. One would not expect such quantities such as kinetic energy distributions, angular distributions or internal energy distributions to necessarily be the same as those for atomic bombardment. In fact, the kinetic energy distributions for Ag and Ag_2 have been shown to be different for Ga and C_{60} bombardment^{21, 24}. The full ramifications of this new physics have yet to be identified.

The other important factor in the new physics is the energy per incident particle. For C_{60} at 15 keV, each C atom only has 250 eV of kinetic energy. The penetration depth is subsequently less for C_{60} than Ga. The concept of energy per particle is essential when analyzing different cluster beams. For example, the metal trimers Au_3 and Bi_3 at 15 keV have 5 keV of kinetic energy per particle.

2.2. *Non-roughening*

A notorious problem with depth profiling with atomic beams is the significant roughening of the surface. From the picture in Figure 2 of the crater formed by the C_{60} , the nagging question occurs as to whether C_{60} bombardment will cause an even worse topological nightmare during depth profiling experiments. Several simulations have been performed by Postawa on systems with a crater, step-edge, or cone²⁵. The C_{60} bombardment is making the surface smoother rather than rougher. Similar observations have been made for bombardment by large Ar clusters²⁶ and they are being commercially developed as a means to make surfaces smoother.

2.3. *Molecular Substrates*

The discussion above is based on simulations on a Ag substrate. The substrates of most interest, however, are soft materials consisting of first row elements like C, O, N and H. Previous simulations of C_{60} bombardment of diamond and graphite have shown similar crater type formation²⁷. Simulations are underway for C_{60} and Au_3 bombardment on ice²⁸ as well as C_{60} on benzene substrates²⁹. The C_{60} bombardment of water ice at 20 keV clearly forms a crater, although because of the mass difference between water and Ag, the carbon atoms can penetrate deeper into the sample. In contrast to the approximately 2-3 nm deep craters formed by C_{60} bombardment of Ag, the crater in ice is closer to 10 nm²³.

The natural question is what is the difference between Au_3 and C_{60} bombardment on these soft materials consisting of elements with relatively light masses? A simple beginning physics analysis would argue that the light C, O and N atoms are unable to effectively stop the heavy Au atoms, especially when they have several thousand eV of kinetic energy. The results so far for Au_3 bombardment on ice²⁸ follow the simple kinematic argument with the Au atoms implanting in the ice substrate.

2.4. *Ionization*

The issue of ionization in SIMS is always a thorny one both experimentally and theoretically. Recently, we have developed a model for collision-induced dissociation³⁰ of water into the ions OH and H^+ . Initial simulations of a single C atom bombarding at 300 eV onto a water slab predict that

one water molecule will be dissociated into ions. For C_{60} bombardment, one simple extrapolation is that as many as 60 protons could be formed. The ramifications of dissociation of water into ions as a means of chemical ionization will be discussed below.

3. An Experimental Point of View

3.1. Implications of the properties of cluster SIMS for auxiliary characterization techniques

The high sputtering yields and applications to molecular depth profiling suggest that additional tools are required to fully characterize molecular solids exposed to extensive bombardment. In our laboratory, the quartz crystal microbalance (QCM) and the atomic force microscope are invaluable aids in determining yields, examining topography, and determining sample film thickness. A typical QCM (Maxtek Inc.) may be modified and mounted directly onto the SIMS sample holder and can measure mass changes of a few ng, yielding film thickness accuracy of about 1 Å. The AFM is capable of determining surface roughness to 3 Å sensitivity and can accurately determine craters that are several microns deep. Most importantly, a maximum field of view of 800 μm by 800 μm can be obtained with this AFM, dimensions large enough to encompass typical SIMS craters.

3.2. The special properties of cluster SIMS

We feel there are 6 important properties of cluster SIMS that, when taken together, present unique opportunities for high sensitivity and high spatial resolution experiments. These properties include:

1. Enhanced sputtering yields, particularly of biological materials
2. Enhanced molecular ion yields, particularly at high mass
3. Reduced topography and reduced interface mixing
4. Enhanced surface sensitivity and depth resolution
5. Molecular depth profiling feasible in some cases
6. Three-dimensional imaging feasible in some cases

In this section we comment on our level of understanding of each of these characteristics, particularly as applied to organic and bio-organic materials.

As noted above, the computer simulations suggest that on metal surfaces, the yields of neutral species are typically enhanced by a factor of 10 or more over corresponding atomic bombardment experiments^{20, 21}. Moreover, the yields themselves can be several hundred particles per impact event. For materials of biological interest, similar trends are emerging. We have performed a number of experiments with water-ice, since it is obviously an important matrix for cell culture and biological material preparation. Using the QCM to determine the amount of ice that is condensed onto a metal surface, it is possible to obtain accurate measurements of the amount of ice that is removed during bombardment. Results for several projectiles are shown in Table I. Details of how these measurements were performed may be found elsewhere³¹.

	Au^+	Au_2^+	Au_3^+	C_{60}^+
Number of H_2O Equivalents Removed	100	575	1190	2510

Table 1. Removed number of water molecule equivalents from an ice film for several different primary ions.

For a weakly bound material such as water-ice, note that there is a 25-fold enhancement in yield when comparing Au^+ and C_{60}^+ , a value typical of metallic systems. The extremely high rate of removal of water molecules with C_{60}^+ , however, is unusual, and may result in some novel desorption mechanisms.

Although the enhancement of the sputtering yield of neutral species is impressive, the situation relative to the enhancement of ion yields is not as clear. For the case of organic thin films produced by Langmuir-Blodgett techniques, the results suggest that the enhancement in the ion yield occurs primarily in the neutral channel as noted above¹³. For the case of higher molecular weight molecules such as small peptides, enhancement factors of several thousand or more are common^{11,32}, and it is difficult to understand how these observations can be explained by kinematic motion alone. In these cases, it is clear that secondary ion formation occurs with much higher efficiency.

There are clues to the origin of this effect. Preliminary computer simulations on ice show that cluster bombardment is effective at dissociating water molecules and that a large number of protons can be produced in the region of the impact event³⁰. Moreover, during the sputtering of ice, it is observed that the ratio of m/z 19 (H_3O^+) to m/z 18 (H_2O^+) increases by about a factor of ten³¹. Hence, there is mounting evidence that cluster beams are prodigious producers of protons in the disrupted region and that this environment could easily enhance the secondary ion yield by chemical ionization through proton attachment. It will be interesting to test this hypothesis further by, for example, comparing the secondary ion yield enhancement for acidic and basic molecules.

For depth profiling and other three-dimensional experiments with cluster beams, it is essential to know whether the erosion process roughens the material as is often seen with atomic bombardment. For metallic systems, it has been shown for a Ni/Cr multilayer stack that the native surface roughness is maintained during erosion¹⁹. This effect is qualitatively predicted by the computer simulations noted earlier, and has been studied extensively using large argon clusters. An exception is bombardment of Si by C_{60}^+ with less than 10 keV of kinetic energy where implantation of the carbon atoms results in the buildup of a carbon-like layer on the surface³³. For organic surfaces, the results so far suggest that cluster beams also produce a smoother surface, without the formation of topography. Preliminary results from Cheng and coworkers on the erosion of trehalose sugar films on Si by AFM measurements have shown roughness values from the eroded surface on the same order of magnitude as from the virgin surface, as shown in Figure 3³⁴. Similar experiments on this system have also suggested that the interface mixing of the trehalose molecules with the Si substrate is on the order of 10 nm or less. Hence, chemical information as a function of depth appears to be retained during erosion with cluster ion beams.

With cluster beams of difference size and momentum now readily available, it should be possible to choose a source that provides a specific information depth of molecules in the near surface region of the sample. To test these ideas, Szakal and coworkers prepared a series of samples with increasing ice film thickness onto a Ag substrate³¹. From the relative intensities of the water peaks to the Ag peaks, they could estimate the escape depths of the underlying Ag atoms. The results of that experiment are summarized in Table 2.

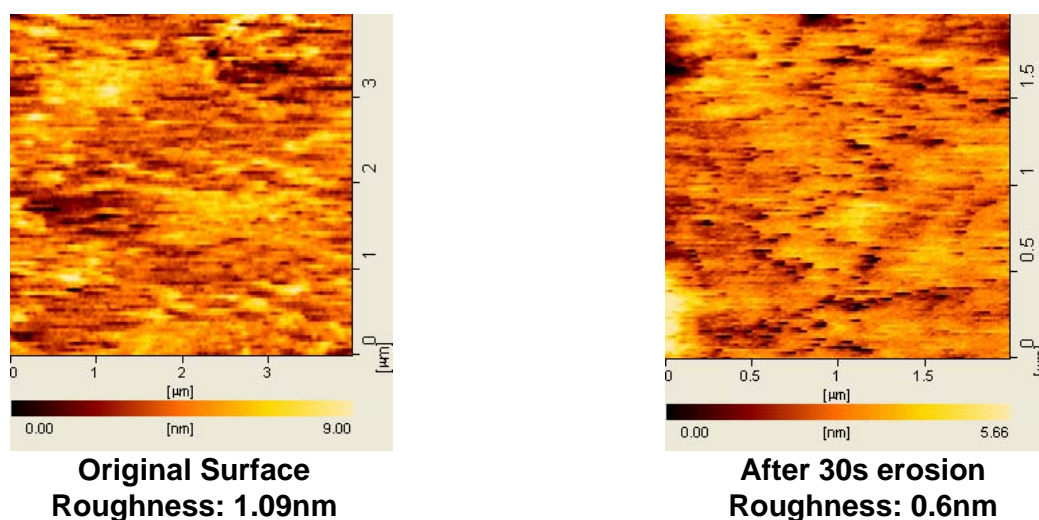


Fig.3. AFM images from original intact trehalose film surface and from surface after 30s C_{60} erosion. Roughness values are as labeled, but note that the field of view sizes are different and the values are not for strict comparison purpose³⁴.

	Au^+	Au_2^+	Au_3^+	C_{60}^+
Escape depth (Å)	26	20	17	6.4

Table 2. Ag secondary ion escape depths when water ice is deposited onto the silver surface³¹.

Details about these experiments are available elsewhere³¹. The results suggest that the larger clusters yield information from closer to the top monolayer than smaller clusters, presumably because the kinetic energy per atom is much lower for the larger cluster.

With high ion yields, low topography and interface mixing, it should be possible to perform molecular depth profiling experiments in a fashion similar to dynamic SIMS studies of elemental species, provided that chemical damage associated with the bombardment does not deplete the signal. Gillen and coworkers have had a great deal of success operating in this mode using SF_5^+ to erode polymer thin films by monitoring fragment ions that are specific to the chemical makeup of the polymer^{17, 35, 36}. Cheng and coworkers have been successful at performing molecular depth profiles of small peptide molecules diluted into the trehalose films mentioned above using C_{60}^+ and Au_3^+ bombardment¹¹. This platform was utilized since the trehalose thin film could be spin-cast onto Si with high uniformity and reproducibility, allowing accurate determination of the erosion rates, sputtering yields and degree of chemical damage. An example of one of their depth profiles is shown in Figure 4.

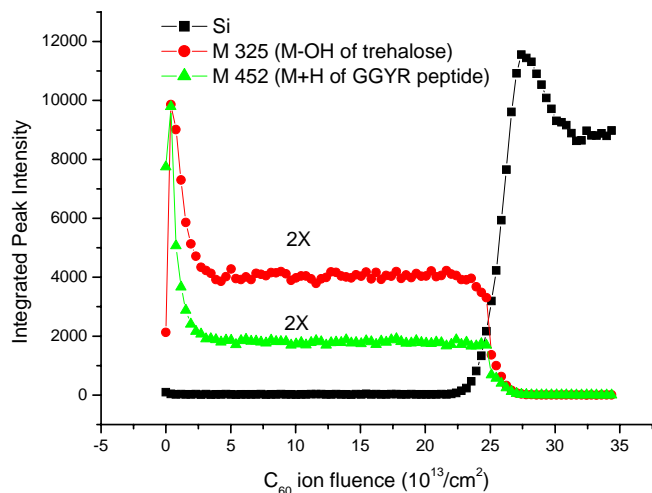


Fig.4. Depth profile of secondary ion intensities versus C_{60}^+ ion fluence of trehalose and GGYR film ($352 \pm 5 \text{ nm}$). Signals are multiplied as indicated on the figure. The film was prepared with a concentration of 1:100 in trehalose¹¹.

The depth profiles are characterized by a fluctuation of signal intensity at the surface, presumably due to changing ionization conditions. Both the trehalose molecular ion and the peptide molecular ion then reach a steady value until the Si interface is reached. All molecular ion signals immediately disappear if the system is interrogated by atomic bombardment. Using the trehalose platform, peptides up to m/z 830 have been successfully examined.

The precise mechanism behind this remarkable effect is not completely clear, but early predictions suggest that the high sputtering yield of trehalose, in this case about 300 molecules per C_{60}^+ projectile, and the low penetration depth of the projectile allow any damage formed during one impact to be removed by subsequent impacts. If this scenario is correct, it is possible that utilization of higher kinetic energy cluster probes might produce even higher quality information. From computer simulations on Ag, for example, it is found that the amount of material removed increases faster than the depth of the damaged layer as the kinetic energy is increased from 5 keV to 20 keV²¹.

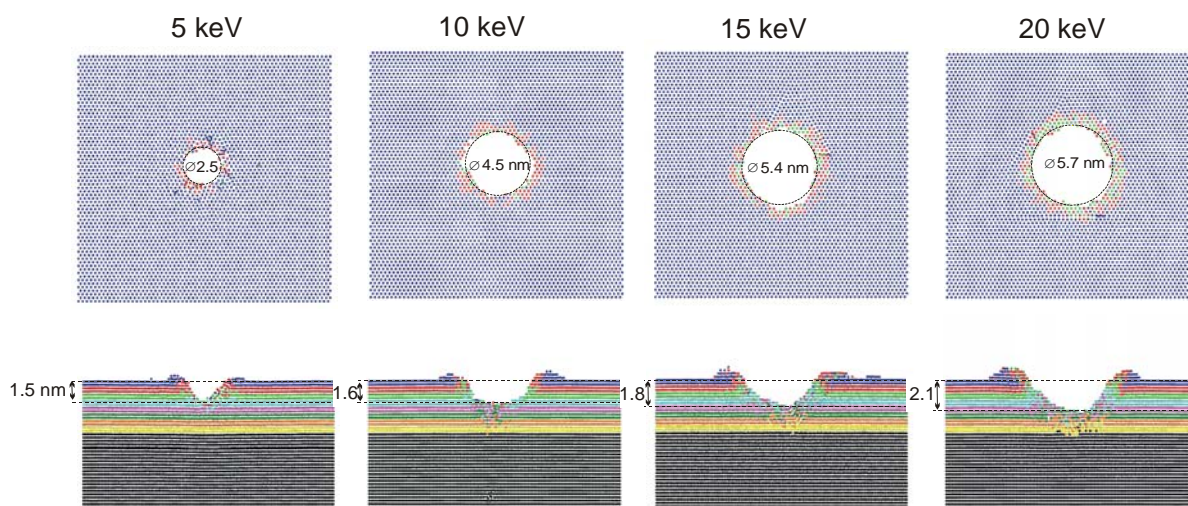


Fig.5. Cross-sectional top and side views of typical craters created by impact of the C_{60} projectile at the $Ag\{111\}$ surface with various kinetic energies at a time of 29.5 ps. The top view shows only atoms that come to rest within ± 0.5 nm of the original surface plane. The crater diameter at the surface is given in each crater. The approximate depth of each crater is shown on the side view²¹.

By putting all of the above properties together, the pieces appear to be in place for successful three-dimensional imaging experiments by utilizing focused cluster ion beams to provide the lateral resolution. These types of experiments are very important since molecule-specific imaging using atomic beams is severely limited by the amount of sample due to the imposition of the static limit. If the same pixel could be interrogated many times, the number of counts could be increased by many orders of magnitude. An example of this effect is shown below where a tetrapeptide (Gly-Gly-Tyr-Arg) has been dissolved in trehalose at 1% concentration and placed as a 300 nm film in an array format on a Si wafer³⁷. In the experiment, 150 nm of the film have been eroded away, and the image recorded. In effect, this image represents the peptide distribution in the middle of the 300 nm film. Moreover, as discussed above, the image can be recorded with a dose that exceeds the static limit, resulting in as many as 30 counts of peptide in each pixel. It will be very exciting to see if these model experiments can be extended to more practical systems.

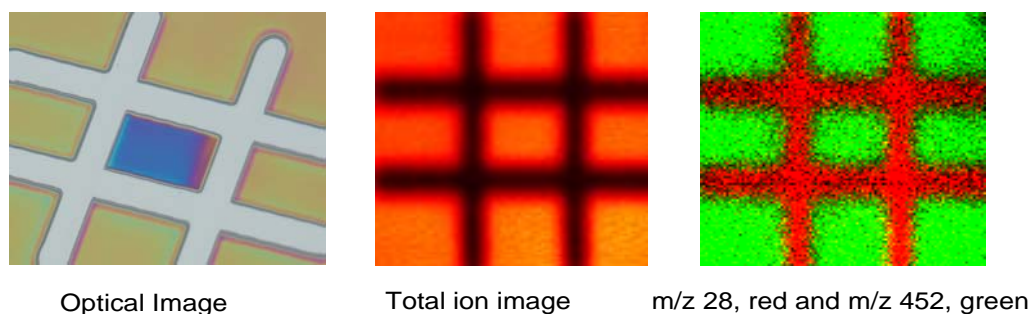


Fig.6. A 300 nm film of Gly-Gly-Try-Arg in array format. The central square has been etched to 150 nm. The change in color in the optical image is due to the interference effect. The field of view is 520 microns³⁷. (The SIMS images on the right were taken before the etch.)

3.3. Which cluster is the best cluster?

With the proliferation of cluster ion sources, it would be useful to be able to rationally select the optimal probe for the experiment at hand. At the moment, commercial sources of SF_5^+ , Au_3^+ , Bi_3^+ and C_{60}^+ are readily available. More specialized probes such as Au_{400}^{4+} are also being investigated³⁸. From the results presented here, it is possible to make a few comments about this issue. We believe that, in general, bigger clusters are better than smaller clusters for yielding the more information in the mass spectra. The reason for this statement, as noted in the first section, is that the energy per particle is smaller, and the deposition of energy near the surface of the material is most efficient. However, there are many other issues to consider. When comparing Au_3^+ or Bi_3^+ to C_{60}^+ , for example, the imaging properties of the metal clusters are much better than C_{60} since they are produced from a liquid metal ion source rather than a gas ion source. These types of ions would be preferred for imaging applications, pending technical advances in C_{60}^+ sources. There is evidence, however, that metal implantation is very efficient for these heavy metal projectiles, so the chemical nature of the sample will be altered in some way during depth profiling experiments. Information depth and yield favors C_{60}^+ , and in general, molecular depth profiling is more effective with the larger projectile. It is possible that large gold clusters or glycerol electrosprayed droplets reported many years ago might be even better³⁹, but for technical reasons, it has not been possible to focus these beams or to use them effectively in a TOF configuration. Perhaps the answer will lie in dual beam experiments – depth profile with C_{60}^+ and image with Au_3^+ or Bi_3^+ .

4. Conclusions

The emergence of cluster SIMS over the last few years has been rapid, and the properties of these probes certainly promise to extend the range of traditional SIMS experiments on organic materials through enhancement of sensitivity and image quality. From a fundamental viewpoint, the properties of the cluster/solid interaction are fascinating to examine. The computer simulations clearly show that the scale of the phenomenon is large relative to atomic bombardment, yet still much smaller than the ablation associated with MALDI. The formation of craters on the mesoscopic scale from the cluster bombardment appears to be an essential part of any new physics associated with their unique properties. We believe that virtually all of the current rules associated with static SIMS need to be carefully reexamined. Sputtering, ionization, and chemical damage mechanisms all need to be examined in much more detail. It is not even clear that the generic form of current TOF-SIMS instrumentation is appropriate for the cluster modality. Fortunately, the field is getting larger, and the number of investigators attacking such issues means we will have better guidelines in very short order. From our view point, the end is not yet in sight.

5. Acknowledgement

The authors acknowledge the National Institutes of Health and the National Science Foundation for partial financial support of this work.

- (1) Lutz, H.; Sitzmann, R. *Physics Letter* **1963**, *5*, 113.
- (2) Maul, J. L.; Schulz, F.; Wittmaack, K. *Rad. Effects* **1973**, *18*, 211.
- (3) Benninghoven, A. *Zeitschrift fuer Physik* **1970**, *230*, 403-417.
- (4) Standing, K. G.; Beavis, R. C.; Ens, W.; Schueler, B. W. *Int. J. Mass Spectrom. Ion Phys.* **1983**, *53*, 125.
- (5) Levi-Setti, R.; Wang, Y. L.; Crow, G. J. *Phys. (Paris)* **1984**, *45*, C9-147.
- (6) Karas, M.; Hillenkamp, F. *Anal. Chem.* **1988**, *60*, 2299-2301.
- (7) Appelhans, A. D.; Delmore, J. E. *Anal. Chem.* **1989**, *61*, 1087-1093.
- (8) SIMS XIII Proceedings, *Appl. Surf. Sci.* **2003**, *203-204*.
- (9) Davies, N.; Weibel, D. E.; Blenkinsopp, P.; Lockyer, N.; Hill, R.; Vickerman, J. C. *Appl. Surf. Sci.* **2003**, *203*, 223-227.

- (10) Wong, S. C. C.; Hill, R.; Blenkinsopp, P.; Lockyer, N. P.; Weibel, D. E.; Vickerman, J. C. *Appl. Surf. Sci.* **2003**, 203-204, 219-222.
- (11) Cheng, J.; Winograd, N. *Anal. Chem.* **2005**, 77, 3651-3659.
- (12) Gillen, G.; Roberson, S. *Rapid Commun. Mass Spectrom.* **1998**, 12, 1303-1312.
- (13) Sostarecz Audra, G.; McQuaw Carolyn, M.; Wucher, A.; Winograd, N. *Anal. Chem.* **2004**, 76, 6651-6658.
- (14) Wucher, A.; Sun, S.; Szakal, C.; Winograd, N. *Anal. Chem.* **2004**, 76, 7234-7242.
- (15) Weibel, D. E.; Lockyer, N.; Vickerman, J. C. *Appl. Surf. Sci.* **2004**, 231-232, 146-152.
- (16) Wagner, M. S. *Anal. Chem.* **2004**, 76, 1264-1272.
- (17) Mahoney, C. M.; Roberson, S.; Gillen, G. *Appl. Surf. Sci.* **2004**, 231-232, 174-178.
- (18) Xu, J.; Szakal, C. W.; Martin, S. E.; Peterson, B. R.; Wucher, A.; Winograd, N. *J. Am. Chem. Soc.* **2004**, 126, 3902-3909.
- (19) Sun, S.; Wucher, A.; Szakal, C.; Winograd, N. *Appl. Phys. Lett.* **2004**, 84, 5177-5179.
- (20) Postawa, Z.; Czerwinski, B.; Szewczyk, M.; Smiley, E. J.; Winograd, N.; Garrison, B. J. *Anal. Chem.* **2003**, 75, 4402-4407.
- (21) Postawa, Z.; Czerwinski, B.; Szewczyk, M.; Smiley, E. J.; Winograd, N.; Garrison, B. J. *J. Phys. Chem. B* **2004**, 108, 7831-7838.
- (22) SIMS XIV Proceedings, *Appl. Surf. Sci.* **2004**, 231-232.
- (23) Wojciechowski, I.; Garrison, B. J., unpublished work
- (24) Sun, S.; Szakal, C.; Smiley, E. J.; Postawa, Z.; Wucher, A.; Garrison, B. J.; Winograd, N. *Appl. Surf. Sci.* **2004**, 231-232, 64-67.
- (25) Postawa, Z., unpublished work
- (26) Nakai, A.; Aoki, T.; Seki, T.; Matsuo, J.; Takaoka, G.; Yamada, I. *Nucl. Instrum. Methods Phys. Res., Sect. B* **2003**, 206, 842-845.
- (27) Webb, R.; Kerford, M.; Way, A.; Wilson, I. *Nucl. Instrum. Methods Phys. Res., Sect. B* **1999**, 153, 284-291.
- (28) Russo, M. F.; Wojciechowski, I. A.; Garrison, B. J. *Appl. Surf. Sci.*, SIMS XV, Manchester 2005.
- (29) Smiley, E. J.; Postawa, Z.; Wojciechowski, I. A.; Garrison, B. J. *Appl. Surf. Sci.*, SIMS XV, Manchester 2005.
- (30) Wojciechowski, I.; Garrison, B. J. *J. Phys. Chem. B* **2005**, 109, 2894-2898.
- (31) Szakal, C.; Kozole, J.; Russo, M. F.; Garrison, B. J.; Winograd, N. *Appl. Surf. Sci.*, SIMS XV, Manchester 2005.
- (32) Weibel, D.; Wong, S.; Lockyer, N.; Blenkinsopp, P.; Hill, R.; Vickerman, J. C. *Anal. Chem.* **2003**, 75, 1754-1764.
- (33) Gillen, G., unpublished work
- (34) Cheng, J.; Winograd, N., unpublished work
- (35) Wagner, M. S.; Gillen, G. *Appl. Surf. Sci.* **2004**, 231-232, 169-173.
- (36) Mahoney, C. M.; Roberson, S. V.; Gillen, G. *Anal. Chem.* **2004**, 76, 3199-3207.
- (37) Winograd, N. *Anal. Chem.* **2005**, 77, 142A-149A.
- (38) Tempez, A.; Schultz, J.; Della-Negra, S.; Depauw, J.; Jacquet, D.; Novikov, A.; Lebeyec, Y.; Pautrat, M.; Caroff, M.; Ugarov, M.; Bensaoula, H.; Gonin, M.; Fuhrer, K.; Woods, A. *Rapid Commun. Mass Spectrom.* **2004**, 18, 371-376.
- (39) Cornett, D.; Lee, T.; Mahoney, J. *Rapid Commun. Mass Spectrom.* **1994**, 8, 996-1000.